TISSUE ENGINEERING: Part B
Volume 21, Number 1, 2015

DOI: 10.1089/ten.teb.2014.0180

Imaging Strategies for Tissue Engineering Applications

Seung Yun Nam, PhD,[1,2] Laura M. Ricles, BS,[1] Laura J. Suggs, PhD,[1] and Stanislav Y. Emelianov, PhD[1,2]

Tissue engineering has evolved with multifaceted research being conducted using advanced technologies, and it is progressing toward clinical applications. As tissue engineering technology significantly advances, it proceeds toward increasing sophistication, including nanoscale strategies for material construction and synergetic methods for combining with cells, growth factors, or other macromolecules. Therefore, to assess advanced tissue-engineered constructs, tissue engineers need versatile imaging methods capable of monitoring not only morphological but also functional and molecular information. However, there is no single imaging modality that is suitable for all tissue-engineered constructs. Each imaging method has its own range of applications and provides information based on the specific properties of the imaging technique. Therefore, according to the requirements of the tissue engineering studies, the most appropriate tool should be selected among a variety of imaging modalities. The goal of this review article is to describe available biomedical imaging methods to assess tissue engineering applications and to provide tissue engineers with criteria and insights for determining the best imaging strategies. Commonly used biomedical imaging modalities, including X-ray and computed tomography, positron emission tomography and single photon emission computed tomography, magnetic resonance imaging, ultrasound imaging, optical imaging, and emerging techniques and multimodal imaging, will be discussed, focusing on the latest trends of their applications in recent tissue engineering studies.

Introduction

The field of tissue engineering is evolving continuously, with multifaceted research being conducted using advanced technologies from various fields including engineering, molecular biology, synthetic chemistry, pharmaceutics, and medicine. As a result, tissue engineering has progressed beyond *in vitro* and animal studies, and is rapidly advancing toward clinical applications. As tissue engineering technology matures, it proceeds toward nanoscale strategies for material construction.[1–3] Therefore, to assess advanced applications related to tissue engineering, tissue engineers need versatile imaging methods capable of monitoring not only morphological but also functional and molecular information. Numerous tissue engineering studies still utilize conventional tools, such as histological techniques, which provide important but limited information, especially in the case of *in vivo* preclinical and clinical approaches.[4] Visualizing tissue-engineered constructs using these conventional methods requires destruction of the samples, meaning that longitudinal three-dimensional (3D) volumetric assessment is extremely limited. Also, due to destructive procedures and limited views within the confined volume, histology requires statistical analysis to compensate for inconsistencies of experimental results at various time points and from different samples. However, there are many advanced imaging techniques available for tissue engineers, and an increasing number of recent tissue engineering studies have begun to explore the applications of various advanced imaging modalities.[5–7] Advanced imaging techniques allow for noninvasive, longitudinal, and consistent monitoring of tissue-engineered constructs, thus overcoming limitations of the conventional tools.

The ideal imaging tool for tissue engineering must be applicable from the subcellular level to animal and human studies using safe, quantitative, and noninvasive monitoring (Fig. 1). Therefore, to support all the diverse applications, the ideal imaging technology must have the ability to resolve signals at the subcellular scale and to penetrate through the whole body. Moreover, the imaging tool ideally needs to offer contrast to display all the necessary information covering morphological, physiological, and molecular changes. However, practically there is no single imaging modality that is suitable for all applications and information for tissue-engineered constructs.

All medical imaging systems available for tissue engineering are based on the physical interaction between an internal or external energy source (electromagnetic waves, pressure waves, etc.) and the imaged object (tissues, organs, cells, nanoparticles, molecules, etc.); the imaging systems detect the energy change transmitted from the object to form an image. Hence, specific properties of medical imaging

Departments of [1]Biomedical Engineering and [2]Electrical and Computer Engineering, The University of Texas at Austin, Austin, Texas.

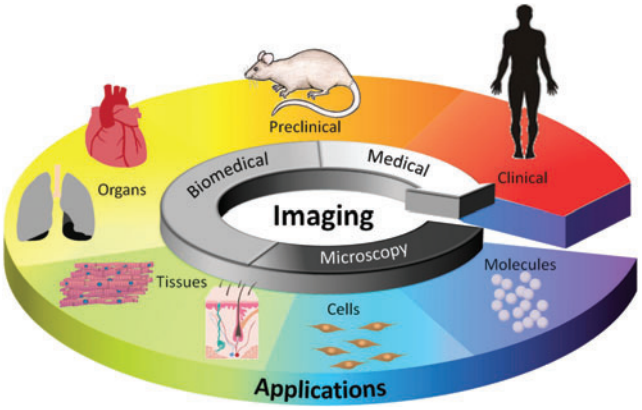

FIG. 1. Illustration for the role of imaging in tissue engineering applications. Color images available online at www.liebertpub.com/teb

methods, such as spatial and temporal resolution, penetration depth, applicable endogenous and exogenous contrast agents, safety, and cost, are determined by the intensity and wavelength of energy sources as well as characteristics of the imaging system (Table 1).[4,8–11] Thus, as briefly presented in Figure 2, each imaging method has its own range of applications and provided information based on the specific properties of the imaging technique. Therefore, according to the requirements of the tissue engineering studies, the most appropriate tool should be selected among a variety of imaging modalities by tissue engineers.

The goal of this review article is to describe available biomedical imaging methods to assess applications related to tissue engineering and to provide tissue engineers with criteria and insights for determining the best imaging strategies. Commonly used biomedical imaging modalities, including X-ray and computed tomography (CT), positron emission tomography (PET) and single photon emission computed tomography (SPECT), magnetic resonance imaging (MRI), ultrasound imaging, optical imaging, and emerging techniques and multimodal imaging, will be discussed, focusing on the latest trends of their applications in recent tissue engineering studies.

Imaging Strategies for Tissue Engineering

X-ray/CT

Radiographic imaging, including X-ray imaging and CT, has been the main diagnostic method since it was invented, and its use has rapidly increased due to excellent spatial resolution and great contrast for visualizing anatomy, especially bone structure.[12,13] The energy source for radiographic imaging is X-ray energy, which is much higher than light energy so that it can penetrate through the human body. Images from X-ray imaging and CT are created by measurement of attenuation of the projected X-ray beam. Due to the high level of the imaging energy source, X-ray imaging and CT has excellent penetration depth, enabling clinical approaches. However, X-ray radiation is ionizing and can damage tissue or samples. In addition, even though X-ray imaging and CT are powerful tools for bone imaging, contrast between soft tissues is not as high as bone. Also, although some researchers have explored functional and

TABLE 1. PROPERTIES OF IMAGING MODALITIES FOR TISSUE ENGINEERING APPLICATIONS

	Micro-PET	*Micro-CT*	*Micro-MRI*	*Micro ultrasound*	*OCT*	*Optical microscopy*	*Bioluminescence*	*Photoacoustics*
Imaging depth	Full body	Full body	Full body	10 mm	1–3 mm	0.3–1.0 mm	10 mm	20 mm
Spatial resolution	1–2 mm	5 μm	5–200 μm	20–100 μm	1–15 μm	0.2–1 μm	2–3 mm	50–150 μm
Real-time	No	No	Yes	Yes	Yes	Yes	Yes	Yes
Anatomy	Poor	Excellent	Excellent	Very good	Good	Poor	Poor	Good
Endogenous contrast: blood	Poor	Poor	Very good	Good	Poor	Very good	Poor	Excellent
Endogenous contrast: bone	Good	Excellent	Very good	Poor	Good	Very good	Poor	Poor
Blood perfusion	Poor	Poor	Excellent	Good	Poor	Poor	Poor	Excellent
Oxygen saturation	Poor	Poor	Very good	Poor	Poor	Poor	Poor	Excellent
Molecular imaging using contrast agents	Excellent	Poor	Very good	Good	Good	Excellent	Excellent	Excellent
Cost	High	Medium	High	Low	Low	Low	Low	Medium
Portability	Low	Low	Low	High	High	High	High	High

Adapted from Refs.[4,8–11]
CT, computed tomography; MRI, magnetic resonance imaging; PET, positron emission tomography; OCT, optical coherence tomography.

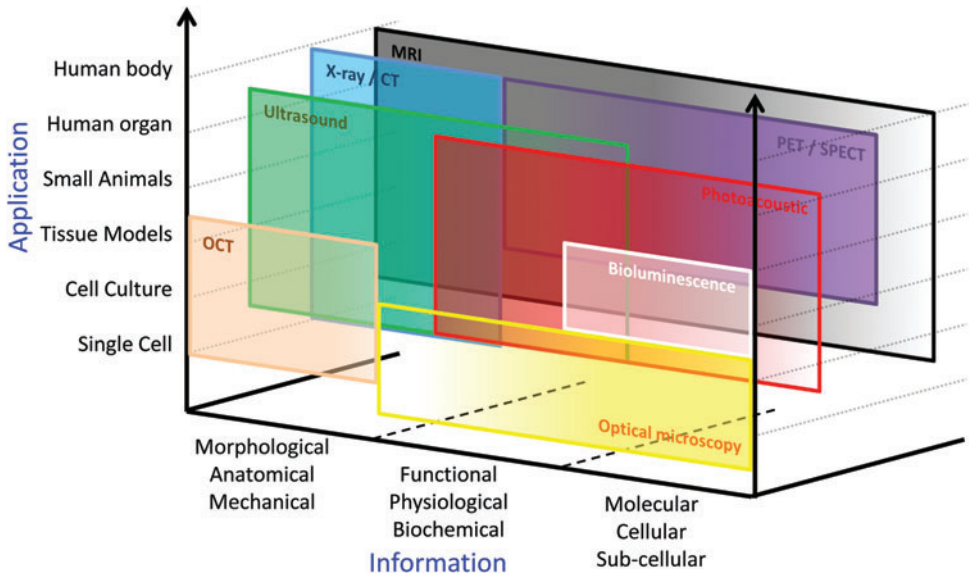

FIG. 2. Available applications and information for various imaging modalities. CT, computed tomography; MRI, magnetic resonance imaging; OCT, optical coherence tomography; PET, positron emission tomography; SPECT, single photon emission computed tomography. Color images available online at www.liebertpub.com/teb

molecular imaging with X-ray imaging and CT, contrast agents are still limited compared to other molecular imaging techniques.

CT, including micro-CT, and X-ray are commonly used to assess therapies aimed at healing bone defects by monitoring the morphological changes in the bone over time.[14–16] Bone has highly absorbing properties, and thus new bone deposition can be imaged using X-ray-based modalities. In addition, *in vivo* and *ex vivo* analysis of bone ingrowth and integration into porous scaffolds can be monitored with CT and X-ray imaging technologies. The evaluation of bone ingrowth into various scaffolds has been demonstrated.[16–18] In one study, the mineralization stages at different distances from the scaffold interface were monitored using X-ray and provided insight into the complicated mineral deposition steps at the organic-mineral interface.[17] Also, micro-CT has been employed to evaluate the optimal culture conditions for bone mineralization of various scaffolds *in vitro*.[19] Human mesenchymal stem cells were cultured in scaffolds of different materials and under static or perfused medium flow conditions.[19] The resulting spatial distribution and interconnectivity of bone formation were visualized using micro-CT.[19] Thus, this technique provided information to optimize the culture conditions to enhance the osteogenic behavior of mesenchymal stem cells and bone formation.

X-ray and CT imaging techniques have also been used to assess the properties of tissue-engineered constructs, including porosity, pore size, and interconnectivity.[20–22] A commonly used contrast agent for CT imaging is Hexabrix, and many have used Hexabrix to coat scaffolds to enhance the contrast necessary for micro- or nano-CT imaging. Silk fibroin scaffolds prepared by different synthesis techniques and seeded with chondrocytes were cultured *in vitro* and imaged with Hexabrix-enhanced micro-CT to evaluate proteoglycan production and determine optimal scaffold production conditions for cartilage tissue engineering purposes, as shown in Figure 3A.[20] However, a problem with some of the contrast agents employed for CT imaging of tissue-engineered scaffolds is the potential loss of information. When comparing CT contrast agents Hexabrix and phosphotungstic acid (PTA) with standard techniques for evaluating scaffolds, some discrepancies were discovered.[21] Under certain conditions PTA did not sufficiently coat the entire matrix, resulting in false void space being depicted in the CT images.[21] However, in general, nano-CT imaging quite accurately showed the ECM being deposited only around the periphery of the scaffold, whereas other conventional techniques that are depth-limited could result in the misinterpretation of scaffolds being fully composed of ECM.[21] To overcome the use of contrast agents, which may be toxic and require fixation of the samples, X-ray phase-contrast micro-CT imaging can be performed. Phase-contrast X-ray imaging is sensitive to light elements, which are commonly found in tissue, and thus it overcomes the disadvantage of conventional X-ray imaging, which is not capable of imaging soft tissue because of poor contrast.[22] This imaging technique has been used to visualize cells seeded on poly(lactic-*co*-glycolic) acid (PLGA) scaffolds and monitor the rate in which the cells modify the scaffolds overtime.[22]

Many have also attempted to visualize vasculature using contrast-enhanced CT.[23,24] Radiopaque contrast agents, such as barium sulfate or Microfil, are injected into the vasculature of the animal prior to sacrifice to allow for *ex vivo* imaging of the samples. One study evaluated the vascular ingrowth within a gel system consisting of an arteriovenous loop placed in a particulated porous hydroxyapatite and β-tricalcium phosphate matrix with and without incorporation of exogenous growth factors.[25] Micro-CT analysis was performed with Microfil contrast enhancement to visualize the 3D geometry of the vascular tree within the construct (Fig. 3B), allowing for easy and accurate quantification compared to 2D histological analysis. However, the authors mention that the resolution of the micro-CT scanner, as well as complete filling of the vessels by contrast agent, are limitations in image analysis and could lead to inaccuracies in quantification. Another study compared micro-CT analysis to conventional methods for assessing vessel ingrowth into porous scaffolds.[23] The scaffolds were conjugated with vascular endothelial growth factor (VEGF) to allow gradual release over time. A similar level of vascularization within the VEGF-treated scaffolds was determined when comparing

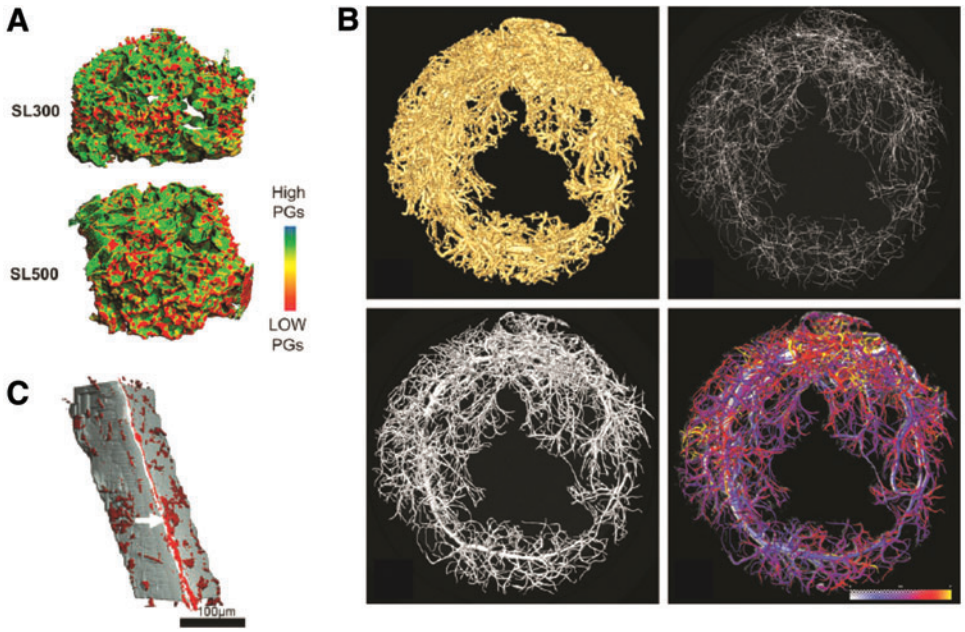

FIG. 3. X-ray and CT images of various tissue-engineered scaffolds. **(A)** Micro-CT analysis of proteoglycan production by chondrocytes seeded in various fibroin scaffolds using Hexabrix contrast agent enhancement. Reprinted with permission from Wang *et al.*[20] **(B)** Three-dimensional reconstructed micro-CT images of vessel ingrowth within a gel system consisting of an arteriovenous loop placed in a particulated porous hydroxyapatite and β-tricalcium phosphate matrix with and without incorporation of exogenous growth factors. Reprinted with permission from Arkudas *et al.*[25] **(C)** Synchroton radiation CT imaging of polyurethane scaffolds seeded with endothelial cells and labeled with anti-CD34-biotin antibodies and FeO-streptavidin particles. Reprinted with permission from Thimm *et al.*[26] Color images available online at www.liebertpub.com/teb

micro-CT to other methods, and although micro-CT could quantify vessels almost down to the capillary level, the actual diameters of the vessels detected by micro-CT were overestimated, most likely due to a merging effect of vessels in close proximity.[23]

Due to their inherent limitations, CT and X-ray imaging are mainly effective in assessing structural and morphological information of tissue-engineered constructs. However, recently there have been some trials to visualize cells using X-ray imaging or CT. For example, X-ray imaging has also been used to monitor cell spreading on 3D scaffolds[26] and cell migration *in vivo*.[27] Cells are usually labeled with a metal contrast agent, such as iron oxide or gold nanoparticles, prior to incorporation into the scaffold or delivery *in vivo* so that the cells can be visualized using X-ray imaging. CT imaging was able to visualize the distribution of endothelial cells seeded in 3D polyurethane scaffolds and labeled with iron oxide particles, as shown in Figure 3C.[26] In addition, the *in vivo* distribution of iron oxide-labeled stem cells delivered intra-arterially has been accomplished using micro-CT.[27] Thus, the kinetics and migration of stem cells delivered for therapeutic purposes can potentially be visualized over time using X-ray, providing more information about the progression of diseases and the therapeutic benefits of the stem cells.

Nuclear medicine (PET/SPECT)

Nuclear medicine, which includes PET and SPECT, has been used as a powerful diagnostic tool to evaluate functional and molecular data of the imaged target.[10,28] The fundamental principle underlying PET/SPECT imaging is the use of radioactive agents, which can localize in specific organs or tissue on the basis of their biochemical or physiological properties. Because specific chemicals of biological interest can be radiolabeled, nuclear imaging has the potential to monitor functional processes. Among biomedical imaging modalities available for whole body imaging, PET and SPECT are the main molecular imaging techniques with the highest sensitivity and the various isotopes available as contrast agents. In addition, PET and SPECT have very high sensitivity and there are various isotopes available as contrast agents for these nuclear medicine imaging techniques. However, PET and SPECT are based on the detection of gamma waves from the isotopes and, like X-ray and CT, are thus ionizing. Also, nuclear imaging modalities are expensive and spatial and temporal resolution of nuclear medicine is poor, which limits visualization of tissue- engineered constructs at the sub-millimeter level.

PET and SPECT imaging have been used to track stem and progenitor cells delivered within *in vivo* injury models to monitor the cells' function and approximate localization within the body. The functional capability of cells is commonly assessed by the ability of cells to uptake fluorodeoxyglucose (^{18}F-FDG), which is a glucose analog incorporating the positron-emitting radioactive isotope fluorine-18. Uptake of ^{18}F-FDG is correlated with tissue metabolism. The functional capability of an infarct region following delivery of progenitor cells has been assessed using FDG-PET imaging.[29] In addition, PET and SPECT imaging have also been employed for cells delivered within a scaffold. FDG-PET imaging has been used to functionally

characterize stem cells delivered within critical size bone defects,[30,31] and when combined with CT images, provide information about the structural integrity of the bone. Specifically, PET scanning was able to assess the function integrity of the endothelial vascular lining of the networks, which was supported by the histological results.[31] The osteogenic metabolism of genetically engineered bone marrow-derived mesenchymal stem cells was also evaluated using PET imaging for the repair of critical-size bone defects.[32] The cells were engineered to have sustained expression of bone morphogenetic protein (BMP)2/VEGF, resulting in enhanced osteogenic potential, angiogenesis, and regeneration of bone defects compared with controls, as shown in Figure 4A.[32] In addition, adipose-derived stem cells transfected with BMP2 and VEGF plasmids to promote reconstruction of bone defects were monitored using SPECT imaging.[33]

The release kinetics of growth factors from polymeric scaffolds has also been evaluated using SPECT imaging.[34] BMP2 was labeled with ^{125}I and the *in vitro* and *in vivo* release kinetics from PLGA microparticles was quantified. The scaffolds were implanted into bone defect models and the osteoinductive capacity of the scaffolds was evaluated, including looking at the release kinetics of the growth factor over 28 days.[34] By monitoring the release kinetics, the investigators were able to tailor the scaffold to result in optimal growth factor distribution and healing.

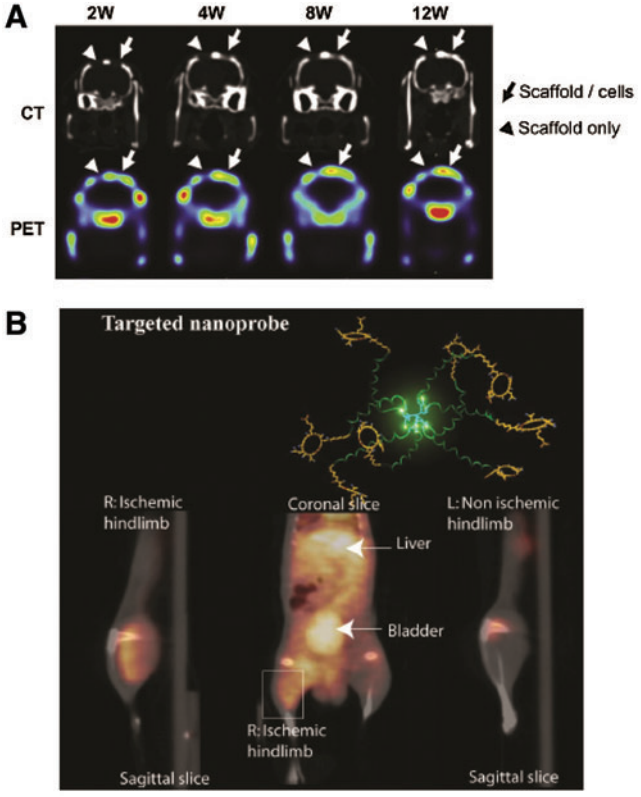

FIG. 4. Nuclear medicine imaging of tissue engineering applications to evaluate wound healing. **(A)** Evaluation of osteogenic metabolism within a bone defect model using PET/CT imaging to assess healing following treatment with poly(lactic-*co*-glycolic) acid (PLGA) scaffolds seeded with bone marrow mesenchymal stem cells. Reprinted with permission from Lin *et al.*[32] **(B)** PET/CT imaging of angiogenesis induced in a hindlimb ischemia model with αvb3 targeted dendritic nanoprobes. Reprinted with permission from van de Almutairi *et al.*[36] Color images available online at www.liebertpub.com/teb

Contrast agents for PET and SPECT imaging have been developed, which target specific biological mechanisms within the body. Specifically for tissue engineering applications, probes targeted to $\alpha_v\beta_3$, a biological marker of angiogenesis, have been developed for noninvasive imaging of angiogenesis.[35,36] One example of these biodegradable probes, developed by Almutairi *et al.*, consists of eight branches functionalized with the radiohalogen ^{76}Br and the targeting peptide RGD at the ends of polymer chains.[36] The nanoprobes showed high specific uptake in angiogenic muscles in an *in vivo* murine hindlimb ischemia model, as shown in Figure 4B.[36] These contrast agents have potential to be used in combination with cell therapies and tissue-engineered scaffolds to monitor the extent of associated angiogenesis.

Magnetic resonance imaging

MRI has been widely applied for both preclinical and clinical applications due to numerous advantages including its excellent imaging penetration depth and safety. When atoms are placed in a strong magnetic field (1.5–10 T), the nuclei, mostly of ^{1}H in the body, are aligned in the direction of the field and the magnetic moment spins around the atom at the Larmor frequency, which is intrinsically related to the material and its environment. By sending and receiving radio frequency pulses, the magnitude and frequency of the magnetization can be measured using coils. According to the pulse sequence, longitudinal or transversal magnetization relaxation times (T1 or T2, respectively) or proton density can be weighted and selectively shown in an MR image. Basically, MRI is a whole body imaging modality with great penetration depth, and micro-MRI can be used by tissue engineers to improve spatial resolution ($\sim$100 μm) in very high (7–9 T) strength magnetic fields. MRI has excellent contrast between various soft tissues. Also, several types of gadolinium- or iron oxide-based contrast agents, including magnetic nanoparticles, are available to enhance contrast and tracking abilities.[37,38] Using contrast from a variety of sources, MRI can provide anatomical, functional, and cellular information. However, although MRI is generally a superior imaging method in many aspects (possibly to be used for molecular imaging as well), it is not the best tool to monitor molecular interactions compared to other molecular imaging modalities mainly due to low sensitivity and limited molecular probes.[28,38]

Because MRI has the superior ability of distinguishing soft tissue contrast, MRI can visualize and assess tissue-engineered constructs without exogenous contrast agents *in vitro* and *in vivo*. Several *in vitro* MRI studies have demonstrated the evaluation of tissue-engineered constructs, such as assessing the composition of bladder acellular matrix-based scaffolds using measured MR relaxation times (T_1, T_2) and diffusion coefficients.[39] MRI has also been used to evaluate intermediate adhesive layers after the integration of hydrogel in cartilage using magnetization relaxation time changes of the scaffolds.[40] In addition, it was demonstrated *in vitro* that changes in MR parameters correlated to cell

behaviors, such as differentiation of mesenchymal stem cells and growth of chondrocytes in the gels.[41,42] As fat tissues have a short T1 relaxation time, resorption of adipose tissue-engineered constructs was longitudinally monitored *in vivo* using MRI.[43] Also, articular cartilage repair in a rabbit osteochondral defect model was monitored over time after thrombin peptide (TP)-508 treatment using quantitative T2 mapping, as shown in Figure 5A.[44]

However, imaging contrast from many cell types could be obscured compared to background and therefore cell tracking using MRI can be challenging, especially after implantation into tissue or scaffolds. Hence, numerous studies in the tissue engineering field incorporated magnetic materials, such as gadolinium or iron oxide, to enhance imaging contrast. Various cell types including astrocytes,[45] chondrocytes (Fig. 5B),[46] and mesenchymal stem cells[47,48] were successfully detected and their localization was visualized within scaffolds or *in vivo* using cell labeling with superparamagnetic iron oxide nanoparticles (SPIONs). Similarly, gadolinium-based magnetic imaging contrast was applied to label endothelial progenitor cells and the labeled cells were intramuscularly injected and successfully tracked in the ischemic rat hindlimb.[49]

Moreover, magnetic material can be used to directly label a scaffold itself to enhance visualizing the morphology of the implanted scaffold. Bone substitutes, such as calcium phosphate cements, were differentiated from bone using incorporation of iron oxide particles incorporated with gadopentetatedimeglumine[50] and gadolinium combined with single-walled carbon nanotubes[51] to overcome MR imaging contrast limitation caused by low hydrogen content in bone and very short T2 relaxation time. In addition, SPIONs have also been used to directly label collagen scaffolds and degradation of the subcutaneously implanted scaffold was clearly visualized *in vivo*.[52] Hydrogel filaments containing gadolinium or SPIO were invented to be visualized by MRI and applied to embolization for the treatment of intracranial aneurysm.[53]

More precise and accurate mechanical properties such as stiffness and elasticity can be assessed using magnetic resonance elastography (MRE), which uses low-frequency shear wave motion generated by an acoustic actuator coupled to the tissue of interest. The acquired shear wave images can be utilized to assess the mechanical property called the shear elastic modulus, presenting the proportionality relationship between lateral stress and strain in a material.[54] Using MRE, nondestructive monitoring and characterization of the osteogenic and adipogenic development of mesenchymal stem cell-based tissue-engineered constructs was demonstrated *in vivo* (Fig. 5C).[55] Also, MRE was able to differentiate the growth stage of engineered fat, which was not possible only with T2 measurements.[56]

MRI is one of the medical imaging techniques most widely and effectively applied for clinical research because of its noninvasiveness and safety. Moreover, morphological, functional, and molecular information can be easily provided together using MRI. Thus, tissue engineers have often used MRI to explore clinical approaches. For instance, morphology of tissue-engineered pulmonary valves implanted in patients as an improvement for pulmonary valve replacement was monitored using MRI and thickening of the wall of the constructs was detected from the patients with graft failure.[57] Neovascularization inside the tissue-engineered constructs, implanted as bone substitutes

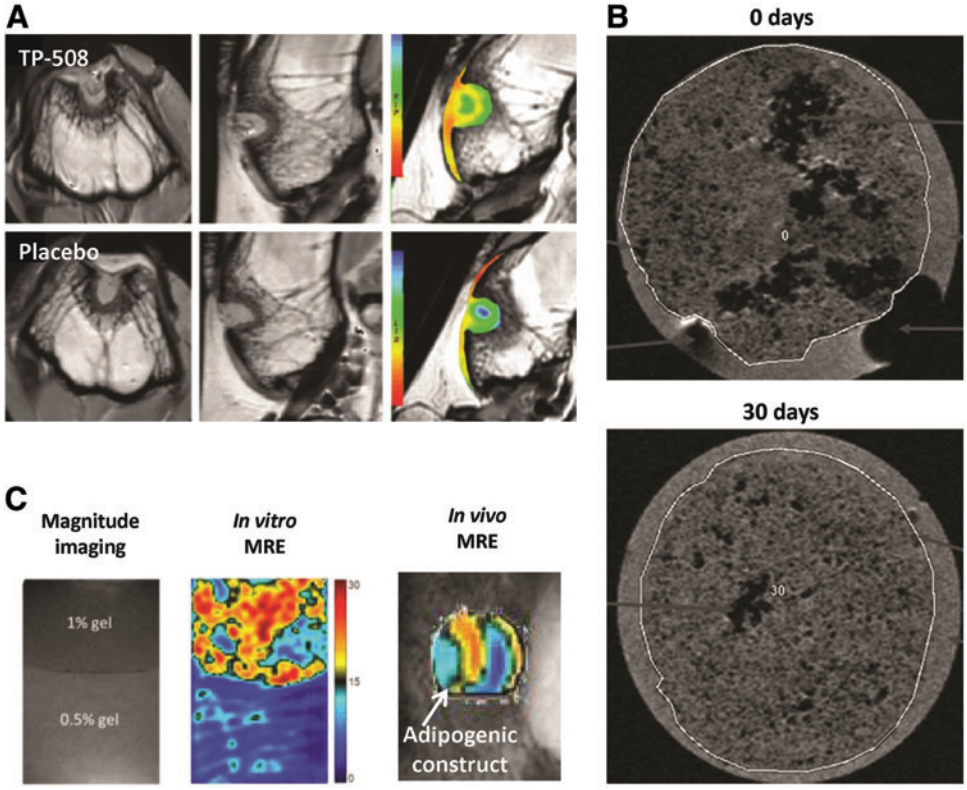

FIG. 5. MR imaging to evaluate tissue-engineered scaffolds and wound healing. **(A)** Cartilage-sensitive MR imaging to evaluate healing within a bone defect model following delivery of thrombin peptide (TP)-508 within PLGA microspheres. Reprinted with permission from Kim *et al.*[44] **(B)** MR imaging of SPIO-labeled chondrocytes seeded in polyvinylidene difluoride hydrogels at 0 and 30 days. Reprinted with permission from Ramaswamy *et al.*[46] **(C)** Nondestructive monitoring of mesenchymal stem cells-based tissue-engineered constructs using high-resolution magnetic resonance elastography (MRE). Reprinted with permission from Othman *et al.*[55] Color images available online at www.liebertpub.com/teb

to augment maxillary sinus, were assessed by dynamic contrast enhanced MRI.[58]

Ultrasound imaging

Ultrasound imaging has been a popular diagnostic technique due to high biocompatibility, excellent temporal resolution, reasonable penetration depth, portability, and low cost.[59] Ultrasound waves are generally transmitted by a single-element or an array transducer, then reflected and backscattered ultrasound waves can be received by the transducer. Penetration depth and spatial resolution of ultrasound imaging are scalable, and thus ultrasound imaging can be used for various applications from small-sized scaffolds to clinical research.

The contrast of conventional ultrasound images originates from the difference in the acoustic impedance, which is determined by the density and bulk moduli of the medium. Therefore, ultrasound imaging can easily offer mechanical and morphological information of tissue-engineered constructs *in vitro* and *in vivo*. Quantitative analysis of gray-scale values of ultrasound scans has been used to evaluate the collagen content of fibrin-based tissue-engineered structures[60] and mineralization in collagen hydrogels (Fig. 6A).[61] Degradation measurements of chondrocyte encapsulated hydrogels were explored *in vitro* by analysis of the speed of sound and slope of attenuation in the gels.[62] Also, using high-frequency ultrasound microscopy, mechanical properties and their localization in the sections of tissue-engineered cartilage were examined after transplantation of the constructs in the subcutaneous areas of nude mice for 2 months.[63] Moreover, ultrasound imaging has been clinically used to evaluate the atherosclerotic evolution in coronary bifurcations after implantation of a bioresorbable scaffold using serial intravascular ultrasound examination.[64] McAllister *et al.* reported the clinical results of mechanical stability and effectiveness of autologous tissue-engineered vascular grafts implanted as arteriovenous shunts in patients with end-stage renal disease.[65]

Conventional ultrasound imaging is effective to visualize basic tissue morphology, but it is highly restricted for quantitative measurement of tissue mechanical properties because the contrast of soft tissue is limited due to a relatively small range of bulk moduli. To overcome the limitation of quantification of tissue mechanical properties, ultrasound elasticity imaging (or ultrasound elastography) can be used. Ultrasound elasticity imaging provides more accurate and quantitative information about the mechanical properties of biological tissue and possibly tissue-engineered constructs.[66–69] Several *ex vivo* studies verified that high-resolution ultrasound microscopy can assess surface irregularities and changes in the morphology and nonlinear elastic properties of engineered oral mucosal tissues.[70–72] In addition, ultrasound elasticity imaging was used for *in vivo* studies to noninvasively assess temporal mechanical property changes in biodegradable polyurethane scaffolds implanted in the rat muscular abdominal wall for up to 12 weeks, as shown in Figure 6B.[73]

In addition to mechanical and morphological properties, functional information can be provided *in vivo* using Doppler ultrasound imaging because Doppler ultrasound imaging is capable of visualizing local fluid flow noninvasively. Also, exogenous contrast agents, mainly microbubbles, can enhance the sensitivity of Doppler ultrasound imaging, so visualization of microvasculature is possible. The function of acellular vascular grafts with engineered collagen-elastin composites implanted in the infrarenal position of the rats was evaluated by measuring blood flood in the graft using Doppler ultrasound imaging.[74] Similarly, blood flow in an allogeneic tissue-

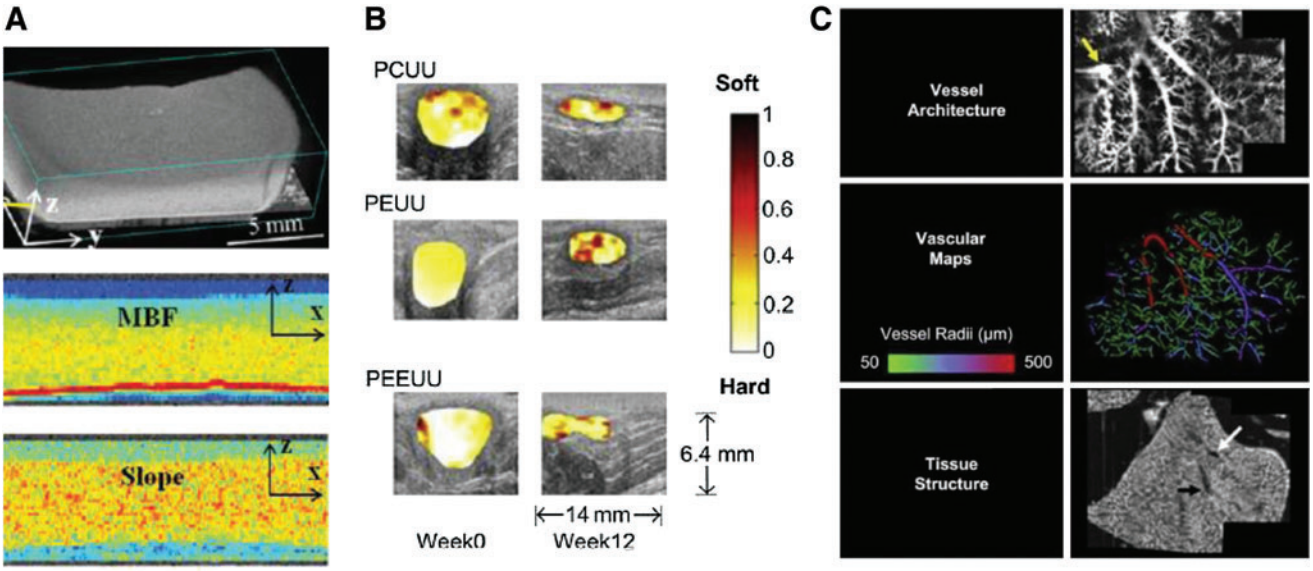

FIG. 6. Ultrasound imaging of 3D scaffolds. **(A)** Characterization of mineral content in collagen hydrogels using high-resolution spectral ultrasound. Reprinted with permission from Gudur *et al.*[61] **(B)** Normalized strain maps laid over B-mode ultrasound images of various polymer scaffolds implanted in abdominal wall defects. Reprinted with permission from Yu *et al.*[73] **(C)** Three-dimensional functional ultrasound imaging of three different liver matrix scaffolds following reseeding with hepatoblast-like cells and bioreactor cultivation to evaluate vascular architecture via contrast infusion. Reprinted with permission from Gessner *et al.*[77] Color images available online at www.liebertpub.com/teb

engineered vascular graft implanted in patients with hemodialysis was monitored over time to assess aneurysm or wall degradation.[75] Doppler ultrasound imaging with injection of air bubbles was applied to demonstrate correct functioning of a tissue-engineered heart valve based on a tubular leaflet design and efficient replacement of the volume in a flow-loop bioreactor.[76] Moreover, microbubbles were injected into extracellular matrix scaffolds to ultrasonically assess flow rates, 3D vessel network architecture, characterization of microvessel volumes and sizes, and delineation of matrix from vascular circuits, as shown in Figure 6C.[77]

Optical imaging

Optical imaging, especially optical and fluorescence microscopy, has been the most commonly used imaging method for tissue engineers with high sensitivity and excellent spatial resolution.[9] Also, various types of biomarkers can be easily used with optical imaging to monitor intracellular signaling and cellular interactions. Therefore, optical imaging is favorable for studies aiming for cellular/molecular information. However, although many advanced optical imaging methods have emerged, most applications of optical imaging methods are restricted by photon scattering, which limits the imaging ability at increasing depth.[59,78]

Due to the penetration limit and invasiveness, optical microscopy has been mostly limited to *in vitro* studies, *ex vivo* verification including histology, or *in vivo* skin models for tissue engineers. Nevertheless, optical microscopy can be the best tool to distinctively visualize and assess molecular functionality of the tissue-engineered constructs owing to excellent spatial resolution, availability of various exogenous and endogenous contrast agents, and great specificity. Therefore, in numerous tissue engineering studies, fluorescence microscopy has been used to distinguish matrix and matrix-embedded cells and examine their functionality.[79–81] In comparison to conventional optical microscopy, two- or multiphoton fluorescence microscopy can reduce optical attenuation and background signals by multiphoton absorption so that depth-resolved validation of the

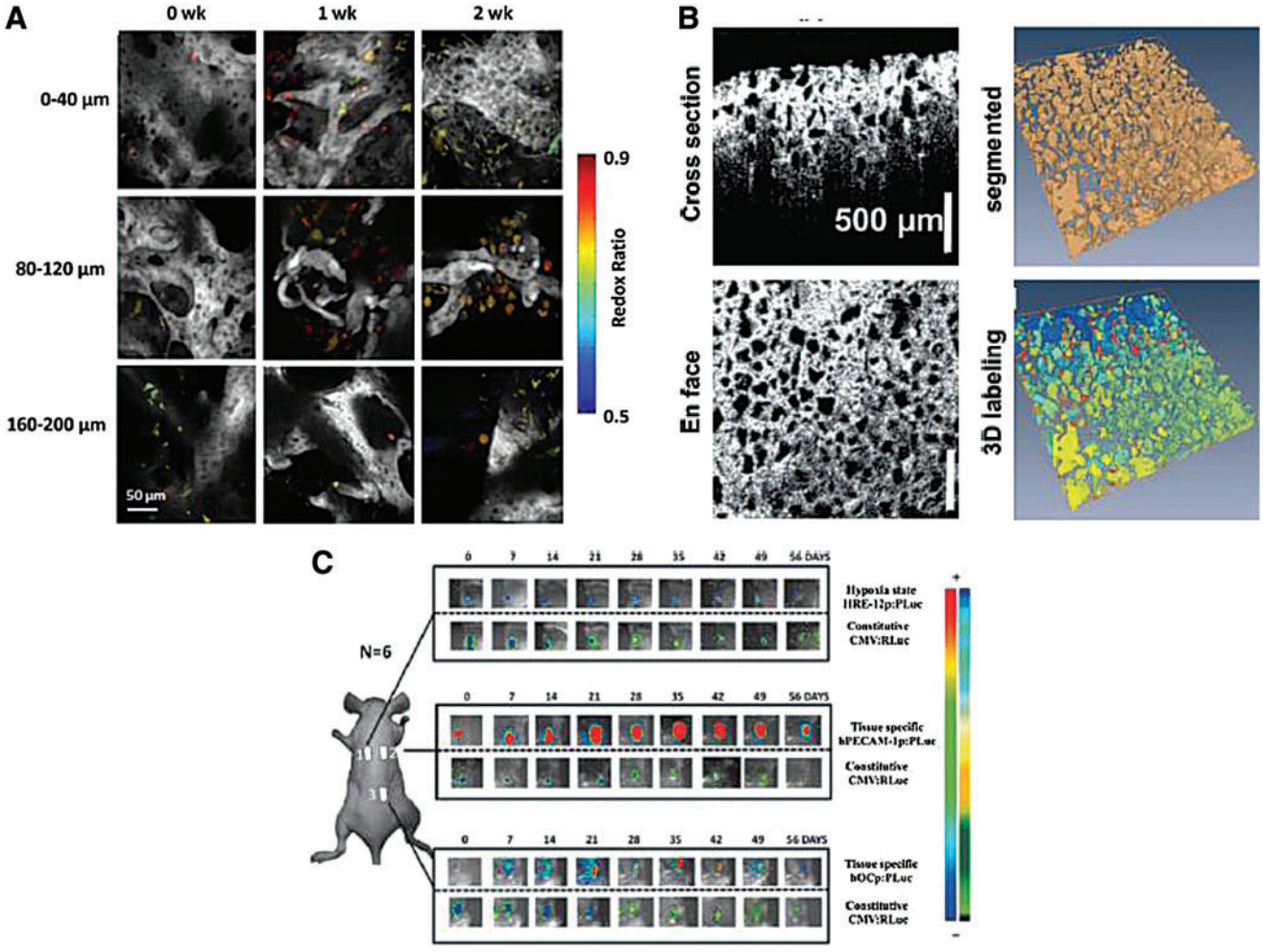

FIG. 7. Optical imaging to evaluate scaffold architecture and cell function. **(A)** *In vitro* tracking of adipose tissue structure during culture within perfusion chambers using two photon excited fluorescence imaging. Reprinted with permission from Ward *et al.*[84] **(B)** OCT imaging to characterize EH-PEG hydrogels fabricated using different formulations in terms of volume porosity, interconnectivity, and pore size. Reprinted with permission from Chen *et al.*[93] **(C)** *In vivo* monitoring of human adipose tissue-derived stromal mesenchymal cell differentiation in subcutaneous implanted demineralized bone matrix scaffolds using bioluminescence imaging. Reprinted with permission from Bago *et al.*[104] Color images available online at www.liebertpub.com/teb

constructs are enabled with the penetration depth increased up to $\sim 500\,\mu m$.[59,82] For instance, two-photon fluorescence microscopy has been successfully applied to visualize the structure of polymer gels and engineered tissue at different depths, even in a bioreactor system (Fig. 7A).[83,84] Also, mesenchymal stem cells embedded in various environments such as silk,[85] chitosan,[86] acellular scaffolds,[87] and rat skin[88] were monitored using two- or multiphoton fluorescence microscopy.

Macroscopic visualization is also available with fluorescence probes emitting in the near-infrared (NIR) region where deeper penetration depth can be achieved with low optical absorption in the tissue.[89] For instance, biodegradable scaffolds containing NIR fluorophores were subcutaneously implanted in mice and longitudinally monitored *in vivo* over 28 days.[90] Moreover, a bone-specific NIR-targeted probe was used to longitudinally visualize mineralization of tissue-engineered osteogenic constructs *in vivo* using NIR fluorescence imaging.[91] However, spatial resolution can be sacrificed by optical scattering and depth-resolved assessment is complicated in macroscopic fluorescence imaging.

Recently, optical coherence tomography (OCT) has been explored as an alternative optical imaging modality for various applications including tissue engineering. OCT is based on interference and coherence between signals reflected from the object and reference signals.[92] Therefore, OCT is more related to optical scattering from tissues than fluorescence or optical absorption, which is adequate to provide anatomical information of the object with sub-millimeter penetration depth. As a result, *in vitro* studies using OCT demonstrated the ability to quantify volume porosity and pore size of macroporous hydrogel scaffolds nondestructively, as shown in Figure 7B.[93] Also, development of tissue-engineered skin was monitored over time using OCT because it does not require sectioning or staining of the samples, as in the case of fluorescence microscopy. In addition, due to its relative noninvasiveness, OCT has been applied to clinical studies, especially including intravascular imaging. For example, longitudinal imaging of neotima formation within patients over 4 years, and visualization of implanted vascular scaffolds, has been performed using OCT.[94–97]

Bioluminescence is another optical imaging technique that uses an internal light source (from luciferin oxidized by luciferase in the presence of ATP and oxygen) in comparison to other optical imaging modalities, which require a light source outside the object.[98,99] Various luciferase reporters can be used and introduced into cells *in vitro*, which can then be incorporated in tissue-engineered constructs and delivered into animals. The emitted light generated from metabolically active cells is detected by an external photon detector with high sensitivity due to very low background noise compared with fluorescence imaging. Therefore, bioluminescence imaging is an excellent method for longitudinal *in vivo* monitoring of cellular information in small animal models, which is hardly achieved by other optical imaging modalities. Specifically, proliferation and osteogenic differentiation of luciferase-labeled mesenchymal stem cells in scaffolds were successfully assessed over several weeks.[100,101] Moreover, using a hypoxia responsive element-luciferase, hypoxia in tissue-engineered constructs was visualized *in vitro* and *in vivo* using bioluminescence imaging.[102] Another study showed the possibility of assessing polymer concentration and structure of tissue-engineered scaffolds by monitoring adenoviral gene expression.[103] In addition, bioluminescence imaging was used for *in vivo* monitoring of differentiation and survival of stem cells labeled with luciferase and green fluorescence protein (Fig. 7C).[104,105] However, in spite of the advantages of bioluminescence imaging, this technique is not appropriate for studies requiring high spatial resolution (better than millimeter level), quantitative analysis, and accurate 3D reconstruction. In addition, bioluminescence imaging is not applicable for clinical applications because of safety issues for bioluminescent reporter genes.[99]

Photoacoustic imaging

In addition to the medical imaging modalities mentioned above, there have been newly emerging imaging technologies to overcome the limitations of former methods. Photoacoustic (PA) imaging is one of the most promising alternative imaging technologies that takes advantage of both ultrasound and optical imaging using the conversion from optical to ultrasonic energy.[59,106–109] Specifically, after nanosecond-laser pulse irradiation, photon energy absorbed in the target in biological tissue temporarily increases temperature and induces thermoelastic expansion.[106–108] The generated acoustic wave can be detected by ultrasound transducers or other sensors with piezoelectric materials. Because ultrasound scattering is about three orders less than optical scattering, the penetration depth of PA imaging can be significantly improved compared with optical microscopy. Also, tradeoffs between the penetration depth and the spatial resolution is controllable depending on the acoustic and optical design of the imaging system, which widens the application range of PA imaging from subcellular to the level of the whole animal.[107] Moreover, unlike ultrasound imaging, various options for endogenous and exogenous contrast agents, such as hemoglobin, melanin, metallic nanoparticles, and dyes, are available in PA imaging so that functional and molecular/cellular information can be provided using blood vessel imaging or labeled cell/protein tracking.[5,109,110]

PA microscopy with subcellular level of spatial resolution within relatively low penetration depth (<1 mm) is a useful tool for *in vitro* 3D nondestructive assessment of tissue-engineered constructs. For instance, tissue-engineered polymer scaffolds implemented with single-walled carbon nanotubes were assessed better than micro-CT in terms of imaging contrast and quantitative analysis of the scaffold structure.[111] Moreover, spatial distribution of various cells inside the tissue-engineered constructs was successfully visualized over time *in vitro* using dyes, gold nanoparticles, or strong endogenous optical absorption of melanoma cells (Fig. 8A).[112–114] *In vivo* animal studies using multiple PA imaging systems have been demonstrated, including a single element transducer-based microscopy, linear array-based imaging, and tomography. With its high spatial resolution and sensitivity, PA microscopy was useful to visualize vascularization and scaffold degradation in the nude mouse ear model as shown in Figure 8B.[115,116] Linear ultrasound array-based PA imaging is capable of detecting a target at deeper regions than PA microscopy and thus can be applied for a rat model, having been commonly used for tissue regeneration studies.[117,118] For example, it was demonstrated that mesenchymal stem cells labeled with gold nanospheres and delivered within

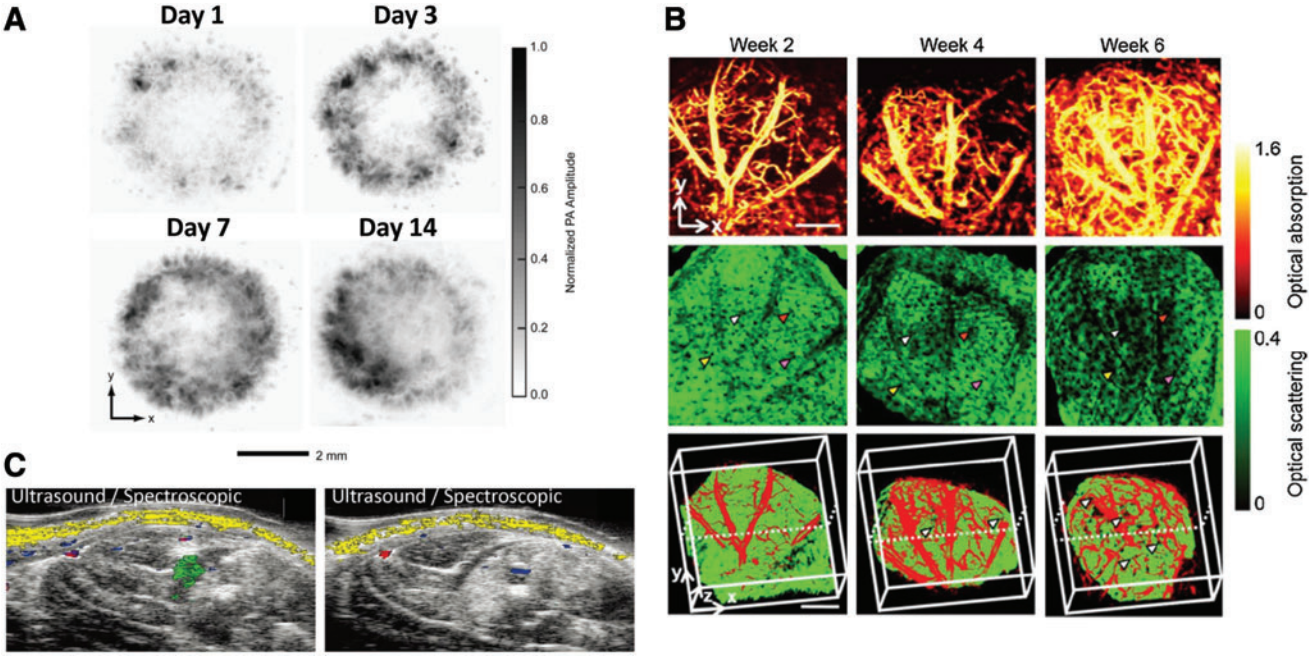

FIG. 8. Photoacoustic imaging to track cells and monitor neovascularization. **(A)** *In vitro* photoacoustic microscopy images to evaluate the distribution of melanoma cells seeded in PLGA inverse opal scaffolds under different culture conditions. Reprinted with permission from Zhang *et al.*[112] **(B)** Optical-resolution photoacoustic microscopy (*top*), OCT (*middle*), and combined (*bottom*) images of neovascularization within inverse opal scaffolds implanted in a mouse ear model. Reprinted with permission from Cai *et al.*[115] **(C)** Combined ultrasound and spectroscopic photoacoustic imaging of gold nanoparticle-labeled mesenchymal stem cells intramuscularly injected within a PEGylated fibrin hydrogel. Reprinted with permission from Nam *et al.*[118] Color images available online at www.liebertpub.com/teb

ischemic muscle in PEGylated fibrin gel can be longitudinally monitored *in vivo* as presented in Figure 8C.[118,119]

Multimodal imaging

As described in Figure 2, each imaging modality has drawbacks and there is not a single imaging modality that is ideal in terms of providing all of the desired information. Consequently, multimodal imaging can be one strategy to overcome limitations of each imaging method and complementarily offer morphological, functional, and molecular information about tissue-engineered constructs. In addition, the multimodal imaging strategy tends to utilize synergetic features of different imaging techniques. Recently, combinations of imaging modalities such as CT/PET, CT/SPECT, MRI/CT, MRI/PET, MRI/fluorescence, ultrasound/PA, and PA/OCT, have been explored for visualization of engineered tissue constructs in preclinical and clinical applications. In addition to effective fusion of imaging systems, contrast agents are also essential for multimodal imaging and various types of multimodal imaging contrast agents have recently been developed.[120,121]

CT/nuclear medicine is one of the most widely used multimodal imaging strategies, especially for clinical use.[32,122] PET/CT or SPECT/CT can be effectively coupled with many shared components, and it can be highly useful for tissue engineering applications because PET and SPECT can provide functional information concerning cellular and tissue function and CT provides structural information about the surrounding tissue.[4,123] For instance, *in vivo* molecular imaging was performed with PET/CT to observe matrix metalloproteinase increase (PET) and corresponding bone formation changes (CT) at different time points after BMP-induced cell injection.[124] Also, migration of ^{111}In-oxine-labeled human mesenchymal stem cells was successfully monitored *in vivo* using SPECT/CT for 48 h after cell implantation in the rat tibia.[125] In addition, MR imaging has been complemented with other imaging methods such as X-ray, PET, and optical imaging. Researchers have investigated the development of magnetic material-based multimodal contrast agents. For example, gold nanoparticles complexed with gadolinium provide contrast for both X-ray and MRI.[126] Moreover, radiolabeling of SPION using ^{64}Cu allowed *in vivo* MRI/PET, and thus drawbacks including low sensitivity for MRI and low spatial resolution for PET were successfully complemented.[127] In addition, extensive studies have been devoted to iron oxide nanoparticles combined with fluorescence or luminescence imaging agents for the dual MRI/optical imaging method.[128–130] PA imaging is another strong candidate for multimodal imaging. It can be effectively combined with ultrasound imaging due to similarities of the two imaging systems, such as transducers and data acquisition units.[106,131] Therefore, fusion of ultrasonically acquired structural data and photoacoustically obtained functional and molecular data can provide synergetic benefits for a variety of applications that require noninvasive monitoring of implanted tissue-engineered constructs.[117,118] Novel dual contrast agents for combined ultrasound and PA imaging have recently been developed by indocyanine green loading to perfluorocarbon nanodroplets.[132] Also, hybrid PA imaging is possible with other optical imaging modalities, such as OCT, by sharing a photon delivery system to complement structural information.[115]

Conclusion

To fully evaluate tissue-engineered constructs and regenerative medicine tools, it is often necessary to employ advanced biomedical imaging technologies. Imaging and subsequent analysis provides information about tissue-engineered scaffolds and regenerating tissue, including morphological changes and functional information, integration with native tissue, growth factor release, cell incorporation within scaffolds and tissue, and the therapeutic benefits offered by these tissue-engineered techniques. This information is desirable on many spatial scales, from subcellular to whole animal analysis, and from applications ranging from *in vitro* to *in vivo*, including clinical applications. While many of the advanced biomedical imaging technologies offer various advantages over conventional techniques, there is not a single imaging modality that provides all of the necessary information. For example, nuclear medicine and optical techniques provide high sensitivity and functional information, but do not provide anatomical information and can suffer from safety concerns or poor imaging depth. On the other hand, radiographic and ultrasound imaging can provide anatomical information with good resolution and imaging depth, but issues with molecular imaging agents limit the types of tissues that can be imaged. Although MRI overcomes many obstacles related to penetration depth and contrast, the low sensitivity, limited number of available molecular probes, and the high cost associated with MR imaging hinder the use of MRI. Thus, researchers are often forced to choose an imaging modality based on the desired information and application, knowing that not all information will be obtained. However, the emergence of multimodal imaging can help overcome the drawbacks from individual imaging technologies by combining the desirable properties of various imaging modalities. In addition, the development of advanced contrast agents that provide not only enhanced contrast but also functional information has contributed to the advancement of incorporating biomedical imaging and tissue engineering. Overall, imaging technologies can assist in advancing tissue engineering strategies forward and toward clinical applications.

Disclosure Statement

No competing financial interests exist.

References

1. Place, E.S., Evans, N.D., and Stevens, M.M. Complexity in biomaterials for tissue engineering. Nat Mater **8,** 457, 2009.
2. Dvir, T., Timko, B.P., Kohane, D.S., and Langer, R. Nanotechnological strategies for engineering complex tissues. Nat Nanotechnol **6,** 13, 2010.
3. Griffith, L.G., and Naughton, G. Tissue engineering—current challenges and expanding opportunities. Science **295,** 1009, 2002.
4. Appel, A.A., Anastasio, M.A., Larson, J.C., and Brey, E.M. Imaging challenges in biomaterials and tissue engineering. Biomaterials **34,** 6615, 2013.
5. Cai, X., Zhang, Y.S., Xia, Y., and Wang, L.V. Photoacoustic microscopy in tissue engineering. Mater Today **16,** 67, 2013.
6. Appel, A., Anastasio, M.A., and Brey, E.M. Potential for imaging engineered tissues with X-ray phase contrast. Tissue Eng Part B Rev **17,** 321, 2011.
7. Guagliardi, A., Giannini, C., Cedola, A., Mastrogiacomo, M., Ladisa, M., and Cancedda, R. Toward the x-ray microdiffraction imaging of bone and tissue-engineered bone. Tissue Eng Part B Rev **15,** 423, 2009.
8. Pysz, M.A., Gambhir, S.S., and Willmann, J.K. Molecular imaging: current status and emerging strategies. Clin Radiol **65,** 500, 2010.
9. Georgakoudi, I., Rice, W.L., Hronik-Tupaj, M., and Kaplan, D.L. Optical spectroscopy and imaging for the noninvasive evaluation of engineered tissues. Tissue Eng Part B Rev **14,** 321, 2008.
10. Rahmim, A., and Zaidi, H. PET versus SPECT: strengths, limitations and challenges. Nucl Med Commun **29,** 193, 2008.
11. Massoud, T.F., and Gambhir, S.S. Molecular imaging in living subjects: seeing fundamental biological processes in a new light. Genes Dev **17,** 545, 2003.
12. Brenner, D.J., and Hall, E.J. Computed tomography—an increasing source of radiation exposure. N Engl J Med **357,** 2277, 2007.
13. Fleischmann, D., and Boas, F.E. Computed tomography—old ideas and new technology. Eur Radiol **21,** 510, 2011.
14. Zhang, X., Xie, C., Lin, A.S., Ito, H., Awad, H., Lieberman, J.R., Rubery, P.T., Schwarz, E.M., O'Keefe, R.J., and Guldberg, R.E. Periosteal progenitor cell fate in segmental cortical bone graft transplantations: implications for functional tissue engineering. J Bone Miner Res **20,** 2124, 2005.
15. Grayson, W.L., Fröhlich, M., Yeager, K., Bhumiratana, S., Chan, M.E., Cannizzaro, C., Wan, L.Q., Liu, X.S., Guo, X.E., and Vunjak-Novakovic, G. Engineering anatomically shaped human bone grafts. Proc Natl Acad Sci U S A **107,** 3299, 2010.
16. Cowan, C.M., Shi, Y.-Y., Aalami, O.O., Chou, Y.-F., Mari, C., Thomas, R., Quarto, N., Contag, C.H., Wu, B., and Longaker, M.T. Adipose-derived adult stromal cells heal critical-size mouse calvarial defects. Nat Biotechnol **22,** 560, 2004.
17. Campi, G., Ricci, A., Guagliardi, A., Giannini, C., Lagomarsino, S., Cancedda, R., Mastrogiacomo, M., and Cedola, A. Early stage mineralization in tissue engineering mapped by high resolution X-ray microdiffraction. Acta Biomater **8,** 3411, 2012.
18. Jones, A.C., Milthorpe, B., Averdunk, H., Limaye, A., Senden, T.J., Sakellariou, A., Sheppard, A.P., Sok, R.M., Knackstedt, M.A., Brandwood, A., Rohner, D., and Hutmacher, D.W. Analysis of 3D bone ingrowth into polymer scaffolds via micro-computed tomography imaging. Biomaterials **25,** 4947, 2004.
19. Meinel, L., Karageorgiou, V., Fajardo, R., Snyder, B., Shinde-Patil, V., Zichner, L., Kaplan, D., Langer, R., and Vunjak-Novakovic, G. Bone tissue engineering using human mesenchymal stem cells: effects of scaffold material and medium flow. Ann Biomed Eng **32,** 112, 2004.
20. Wang, Y., Bella, E., Lee, C.S., Migliaresi, C., Pelcastre, L., Schwartz, Z., Boyan, B.D., and Motta, A. The synergistic effects of 3-D porous silk fibroin matrix scaffold properties and hydrodynamic environment in cartilage tissue regeneration. Biomaterials **31,** 4672, 2010.
21. Papantoniou, I., Sonnaert, M., Geris, L., Luyten, F.P., Schrooten, J., and Kerckhofs, G. Three-dimensional characterization of tissue-engineered constructs by contrast-

enhanced nanofocus computed tomography. Tissue Eng Part C Methods **20,** 177, 2014.
22. Giuliani, A., Moroncini, F., Mazzoni, S., Belicchi, M.L., Villa, C., Erratico, S., Colombo, E., Calcaterra, F., Brambilla, L., Torrente, Y., Albertini, G., and Bella, S.D. Polyglycolic acid-polylactic acid scaffold response to different progenitor cell *in vitro* cultures: a demonstrative and comparative X-ray synchrotron radiation phase-contrast microtomography study. Tissue Eng Part C Methods **20,** 308, 2014.
23. Schmidt, C., Bezuidenhout, D., Beck, M., Van der Merwe, E., Zilla, P., and Davies, N. Rapid three-dimensional quantification of VEGF-induced scaffold neovascularisation by microcomputed tomography. Biomaterials **30,** 5959, 2009.
24. Plouraboue, F., Cloetens, P., Fonta, C., Steyer, A., Lauwers, F., and Marc-Vergnes, J.P. X-ray high-resolution vascular network imaging. J Microsc **215,** 139, 2004.
25. Arkudas, A., Beier, J.P., Pryymachuk, G., Hoereth, T., Bleiziffer, O., Polykandriotis, E., Hess, A., Gulle, H., Horch, R.E., and Kneser, U. Automatic quantitative micro-computed tomography evaluation of angiogenesis in an axially vascularized tissue-engineered bone construct. Tissue Eng Part C Methods **16,** 1503, 2010.
26. Thimm, B.W., Hofmann, S., Schneider, P., Carretta, R., and Müller, R. Imaging of cellular spread on a three-dimensional scaffold by means of a novel cell-labeling technique for high-resolution computed tomography. Tissue Eng Part C Methods **18,** 167, 2011.
27. Farini, A., Villa, C., Manescu, A., Fiori, F., Giuliani, A., Razini, P., Sitzia, C., Del Fraro, G., Belicchi, M., and Meregalli, M. Novel insight into stem cell trafficking in dystrophic muscles. Int J Nanomed **7,** 3059, 2012.
28. Dobrucki L.W., and Sinusas, A.J. PET and SPECT in cardiovascular molecular imaging. Nat Rev Cardiol **7,** 38, 2010.
29. Bartunek, J., Vanderheyden, M., Vandekerckhove, B., Mansour, S., De Bruyne, B., De Bondt, P., Van Haute, I., Lootens, N., Heyndrickx, G., and Wijns, W. Intracoronary injection of CD133-positive enriched bone marrow progenitor cells promotes cardiac recovery after recent myocardial infarction: feasibility and safety. Circulation **112,** I178, 2005.
30. Zhou, J., Lin, H., Fang, T., Li, X., Dai, W., Uemura, T., and Dong, J. The repair of large segmental bone defects in the rabbit with vascularized tissue engineered bone. Biomaterials **31,** 1171, 2010.
31. Mertsching, H., Walles, T., Hofmann, M., Schanz, J., and Knapp, W.H. Engineering of a vascularized scaffold for artificial tissue and organ generation. Biomaterials **26,** 6610, 2005.
32. Lin, C.-Y., Chang, Y.-H., Kao, C.-Y., Lu, C.-H., Sung, L.-Y., Yen, T.-C., Lin, K.-J., and Hu, Y.-C. Augmented healing of critical-size calvarial defects by baculovirus-engineered MSCs that persistently express growth factors. Biomaterials **33,** 3682, 2012.
33. Chen, Q.A., Yang, Z.L., Sun, S.J., Huang, H., Sun, X.J., Wang, Z.G., Zhang, Y., and Zhang, B. Adipose-derived stem cells modified genetically *in vivo* promote reconstruction of bone defects. Cytotherapy **12,** 831, 2010.
34. van de Watering, F.C.J., Molkenboer-Kuenen, J.D.M., Boerman, O.C., van den Beucken, J.J.J.P., and Jansen, J.A. Differential loading methods for BMP-2 within injectable calcium phosphate cement. J Control Release **164,** 283, 2012.
35. Jeong, J.M., Hong, M.K., Chang, Y.S., Lee, Y.S., Kim, Y.J., Cheon, G.J., Lee, D.S., Chung, J.K., and Lee, M.C. Preparation of a promising angiogenesis PET imaging agent: Ga-68-labeled c(RGDyK)-isothiocyanatobenzyl-1,4,7-triazacyclononane-1,4,7-triacetic acid and feasibility studies in mice. J Nucl Med **49,** 830, 2008.
36. Almutairi, A., Rossin, R., Shokeen, M., Hagooly, A., Ananth, A., Capoccia, B., Guillaudeu, S., Abendschein, D., Anderson, C.J., Welch, M.J., and Frechet, J.M.J. Biodegradable dendritic positron-emitting nanoprobes for the noninvasive imaging of angiogenesis. Proc Natl Acad Sci U S A **106,** 685, 2009.
37. Jun, Y.W., Lee, J.H., and Cheon, J. Chemical design of nanoparticle probes for high-performance magnetic resonance imaging. Angew ChemInt Ed Engl **47,** 5122, 2008.
38. Terreno, E., Delli Castelli, D., Viale, A., and Aime, S. Challenges for molecular magnetic resonance imaging. Chem Rev **110,** 3019, 2010.
39. Cheng, H.-L.M., Loai, Y., Beaumont, M., and Farhat, W.A. The acellular matrix (ACM) for bladder tissue engineering: a quantitative magnetic resonance imaging study. Magn Reson Med **64,** 341, 2010.
40. Ramaswamy, S., Wang, D.A., Fishbein, K.W., Elisseeff, J.H., and Spencer, R.G. An analysis of the integration between articular cartilage and nondegradable hydrogel using magnetic resonance imaging. J Biomed Mater Res Part B Appl Biomater **77,** 144, 2006.
41. Kotecha, M., Yin, Z., and Magin, R. Monitoring tissue engineering and regeneration by magnetic resonance imaging and spectroscopy. J Tissue Sci Eng S **11,** 2, 2013.
42. Li, W., Hong, L., Hu, L., and Magin, R.L. Magnetization transfer imaging provides a quantitative measure of chondrogenic differentiation and tissue development. Tissue Eng Part C Methods **16,** 1407, 2010.
43. Torio-Padron, N., Paul, D., von Elverfeldt, D., Stark, G., and Huotari, A. Resorption rate assessment of adipose tissue-engineered constructs by intravital magnetic resonance imaging. J Plastic, Reconstr Aesthet Surg **64,** 117, 2011.
44. Kim, M., Foo, L.F., Uggen, C., Lyman, S., Ryaby, J.T., Moynihan, D.P., Grande, D.A., Potter, H.G., and Pleshko, N. Evaluation of early osteochondral defect repair in a rabbit model utilizing Fourier transform–infrared imaging spectroscopy, magnetic resonance imaging, and quantitative T2 mapping. Tissue Eng Part C Methods **16,** 355, 2009.
45. Pickard, M.R., Jenkins, S.I., Koller, C.J., Furness, D.N., and Chari, D.M. Magnetic nanoparticle labeling of astrocytes derived for neural transplantation. Tissue Eng Part C Methods **17,** 89, 2010.
46. Ramaswamy, S., Greco, J.B., Uluer, M.C., Zhang, Z., Zhang, Z., Fishbein, K.W., and Spencer, R.G. Magnetic resonance imaging of chondrocytes labeled with superparamagnetic iron oxide nanoparticles in tissue-engineered cartilage. Tissue Eng Part A **15,** 3899, 2009.
47. Saldanha, K.J., Doan, R.P., Ainslie, K.M., Desai, T.A., and Majumdar, S. Micrometer-sized iron oxide particle labeling of mesenchymal stem cells for magnetic resonance imaging-based monitoring of cartilage tissue engineering. Magn Reson Imaging **29,** 40, 2011.
48. Lalande, C., Miraux, S., Derkaoui, S., Mornet, S., Bareille, R., Fricain, J.-C., Franconi, J.-M., Le Visage, C., Letourneur, D., and Amédée, J. Magnetic resonance imaging tracking of human adipose derived stromal cells within three-dimensional scaffolds for bone tissue engineering. Eur Cells Mater **21,** 341, 2011.
49. Agudelo, C.A., Tachibana, Y., Noboru, T., Iida, H., and Yamaoka, T. Long-term *in vivo* magnetic resonance

imaging tracking of endothelial progenitor cells transplanted in rat ischemic limbs and their angiogenic potential. Tissue Eng Part A **17,** 2079, 2011.
50. Sun, Y., Ventura, M., Oosterwijk, E., Jansen, J.A., Walboomers, X.F., and Heerschap, A. Zero echo time magnetic resonance imaging of contrast-agent-enhanced calcium phosphate bone defect fillers. Tissue Eng Part C Methods **19,** 281, 2013.
51. van der Zande, M., Sitharaman, B., Walboomers, X.F., Tran, L., Ananta, J.S., Veltien, A., Wilson, L.J., Álava, J.I., Heerschap, A., and Mikos, A.G. *In vivo* magnetic resonance imaging of the distribution pattern of gadonanotubes released from a degrading poly (lactic-co-glycolic acid) scaffold. Tissue Eng Part C Methods **17,** 19, 2010.
52. Mertens, M.E., Hermann, A., Bühren, A., Olde-Damink, L., Möckel, D., Gremse, F., Ehling, J., Kiessling, F., and Lammers, T. Iron oxide-labeled collagen scaffolds for non-invasive mr imaging in tissue engineering. Adv Funct Mater **24,** 754, 2014.
53. Killer, M., Keeley, E.M., Cruise, G.M., Schmitt, A., and McCoy, M.R. MR imaging of hydrogel filament embolic devices loaded with superparamagnetic iron oxide or gadolinium. Neuroradiology **53,** 449, 2011.
54. Othman, S.F., Curtis, E.T., Plautz, S.A., Pannier, A.K., Butler, S.D., and Xu, H. MR elastography monitoring of tissue-engineered constructs. NMR Biomed **25,** 452, 2012.
55. Othman, S.F., Curtis, E.T., and Xu, H. *In vivo* magnetic resonance elastography of mesenchymally derived constructs. 2011 International Symposium on IT in Medicine and Education (ITME), 2011, pp. 621.
56. Xu, H., Othman, S.F., and Magin, R.L. Monitoring tissue engineering using magnetic resonance imaging. J Biosci Bioeng **106,** 515, 2008.
57. Voges, I., Bräsen, J.H., Entenmann, A., Scheid, M., Scheewe, J., Fischer, G., Hart, C., Andrade, A., Pham, H.M., and Kramer, H.-H. Adverse results of a decellularized tissue-engineered pulmonary valve in humans assessed with magnetic resonance imaging. Eur J Cardiothorac Surg **44,** e272, 2013.
58. Sauerbier, S., Palmowski, M., Vogeler, M., Nagursky, H., Al-Ahmad, A. Fisch, D., Hennig, J., Schmelzeisen, R., Gutwald, R., and Fasol, U. Onset and maintenance of angiogenesis in biomaterials: *in vivo* assessment by dynamic contrast-enhanced MRI. Tissue Eng Part C Methods **15,** 455, 2009.
59. Ntziachristos, V. Going deeper than microscopy: the optical imaging frontier in biology. Nat Methods **7,** 603, 2010.
60. Kreitz, S., Dohmen, G., Hasken, S., Schmitz-Rode, T., Mela, P., and Jockenhoevel, S. Nondestructive method to evaluate the collagen content of fibrin-based tissue engineered structures via ultrasound. Tissue Eng Part C Methods **17,** 1021, 2011.
61. Gudur, M., Rao, R.R., Hsiao, Y.-S., Peterson, A.W., Deng, C.X., and Stegemann, J.P. Noninvasive, quantitative, spatiotemporal characterization of mineralization in three-dimensional collagen hydrogels using high-resolution spectral ultrasound imaging. Tissue Eng Part C Methods **18,** 935, 2012.
62. Rice, M.A., Waters, K.R., and Anseth, K.S. Ultrasound monitoring of cartilaginous matrix evolution in degradable PEG hydrogels. Acta Biomater **5,** 152, 2009.
63. Tanaka, Y., Saijo, Y., Fujihara, Y., Yamaoka, H., Nishizawa, S., Nagata, S., Ogasawara, T., Asawa, Y., Takato, T., and Hoshi, K. Evaluation of the implant type tissue-engineered cartilage by scanning acoustic microscopy. J Biosci Bioeng **113,** 252, 2012.
64. Lee, I.S., Bourantas, C.V., Muramatsu, T., Gogas, B.D., Heo, J.H., Diletti, R., Farooq, V., Zhang, Y., Onuma, Y., and Serruys, P.W. Assessment of plaque evolution in coronary bifurcations located beyond everolimus eluting scaffolds: serial intravascular ultrasound virtual histology study. Cardiovasc Ultrasound **11,** 25, 2013.
65. McAllister, T. N., Maruszewski, M., Garrido, S.A., Wystrychowski, W., Dusserre, N., Marini, A., Zagalski, K., Fiorillo, A., Avila, H., and Manglano, X. Effectiveness of haemodialysis access with an autologous tissue-engineered vascular graft: a multicentre cohort study. Lancet **373,** 1440, 2009.
66. Garra, B.S. Imaging and estimation of tissue elasticity by ultrasound. Ultrasound Q **23,** 255, 2007.
67. Wells P.N.T., and Liang, H.-D. Medical ultrasound: imaging of soft tissue strain and elasticity. J R Soc Interface **8,** 1521, 2011.
68. Bercoff, J., Tanter, M., and Fink, M. Supersonic shear imaging: a new technique for soft tissue elasticity mapping. IEEE Trans Ultrason Ferroelectr Freq Control **51,** 396, 2004.
69. Deffieux, T., Montaldo, G., Tanter, M., and Fink, M. Shear wave spectroscopy for *in vivo* quantification of human soft tissues visco-elasticity. IEEE Trans Med Imaging **28,** 313, 2009.
70. Winterroth, F., Hollman, K.W., Kuo, S., Izumi, K., Feinberg, S.E., Hollister, S.J., and Fowlkes, J.B. Comparison of scanning acoustic microscopy and histology images in characterizing surface irregularities among engineered human oral mucosal tissues. Ultrasound Med Biol **37,** 1734, 2011.
71. Winterroth, F., Hollman, K.W., Kuo, S., Ganguly, A., Feinberg, S.E., Fowlkes, J.B., and Hollister, S.J. Characterizing morphology and nonlinear elastic properties of normal and thermally stressed engineered oral mucosal tissues using scanning acoustic microscopy. Tissue Eng Part C Methods **19,** 345, 2012.
72. Abraham Cohn, N., Kim, B.-S., Erkamp, R.Q., Mooney, D.J., Emelianov, S.Y., Skovoroda, A.R., and O'Donnell, M. High-resolution elasticity imaging for tissue engineering. IEEE Trans Ultrason Ferroelectr Freq Control **47,** 956, 2000.
73. Yu, J., Takanari, K., Hong, Y., Lee, K.-W., Amoroso, N.J., Wang, Y., Wagner, W.R., and Kim, K. Non-invasive characterization of polyurethane-based tissue constructs in a rat abdominal repair model using high frequency ultrasound elasticity imaging. Biomaterials **34,** 2701, 2013.
74. Kumar, V.A., Caves, J.M., Haller, C.A., Dai, E., Li, L., Grainger, S., and Chaikof, E.L. Acellular vascular grafts generated from collagen and elastin analogues. Acta Biomater **9,** 8067, 2013.
75. Wystrychowski, W., McAllister, T.N., Zagalski, K., Dusserre, N., Cierpka, L., and L'Heureux, N. First human use of an allogeneic tissue-engineered vascular graft for hemodialysis access. J Vasc Surg 2013. DOI: 10.1016/j.jvs.2013.08.018.
76. Weber, M., Heta, E., Moreira, R., Gesché, V., Schermer, T., Frese, J., Jockenhoevel, S., and Mela, P. Tissue-engineered fibrin-based heart valve with a tubular leaflet design. Tissue Eng Part C Methods **20,** 265, 2014.
77. Gessner, R.C., Hanson, A.D., Feingold, S., Cashion, A.T., Corcimaru, A., Wu, B.T., Mullins, C.R., Aylward, S.R.,

Reid, L.M., and Dayton, P.A. Functional ultrasound imaging for assessment of extracellular matrix scaffolds used for liver organoid formation. Biomaterials **34,** 9341, 2013.
78. Luker G.D., and Luker, K.E. Optical imaging: current applications and future directions. J Nucl Med **49,** 1, 2008.
79. Shachar, M., Tsur-Gang, O., Dvir, T., Leor, J., and Cohen, S. The effect of immobilized RGD peptide in alginate scaffolds on cardiac tissue engineering. Acta Biomater **7,** 152, 2011.
80. Lawrence, B.D., Marchant, J.K., Pindrus, M.A., Omenetto, F.G., and Kaplan, D.L. Silk film biomaterials for cornea tissue engineering. Biomaterials **30,** 1299, 2009.
81. Tour, G., Wendel, M., and Tcacencu, I., Human fibroblast-derived extracellular matrix constructs for bone tissue engineering applications. J Biomed Mater Res A **101,** 2826, 2013.
82. Wang, B., König, K., and Halbhuber, K. Two-photon microscopy of deep intravital tissues and its merits in clinical research. J Microsc **238,** 1, 2010.
83. Chalal, M., Ehrburger-Dolle, F., Morfin, I., Vial, J.-C., Aguilar de Armas, M.-R., San Roman, J., Bölgen, N., Piskin, E., Ziane, O., and Casalegno, R. Imaging the structure of macroporous hydrogels by two-photon fluorescence microscopy. Macromolecules **42,** 2749, 2009.
84. Ward, A., Quinn, K.P., Bellas, E., Georgakoudi, I., and Kaplan, D.L. Noninvasive metabolic imaging of engineered 3D human adipose tissue in a perfusion bioreactor. PLoS One **8,** e55696, 2013.
85. Chang, T., Zimmerley, M.S., Quinn, K.P., Lamarre-Jouenne, I., Kaplan, D.L., Beaurepaire, E., and Georgakoudi, I. Non-invasive monitoring of cell metabolism and lipid production in 3D engineered human adipose tissues using label-free multiphoton microscopy. Biomaterials **34,** 8607, 2013.
86. Chen, W.-L., Huang, C.-H., Chiou, L.-L., Chen, T.-H., Huang, Y.-Y., Jiang, C.-C., Lee, H.-S., and Dong, C.-Y. Multiphoton imaging and quantitative analysis of collagen production by chondrogenic human mesenchymal stem cells cultured in chitosan scaffold. Tissue Eng Part C Methods **16,** 913, 2010.
87. Yang, Q., Peng, J., Guo, Q., Huang, J., Zhang, L., Yao, J., Yang, F., Wang, S., Xu, W., and Wang, A. A cartilage ECM-derived 3-D porous acellular matrix scaffold for *in vivo* cartilage tissue engineering with PKH26-labeled chondrogenic bone marrow-derived mesenchymal stem cells. Biomaterials **29,** 2378, 2008.
88. Zhuo, S., Chen, J., Xie, S., Fan, L., Zheng, L., Zhu, X., and Jiang, X. Monitoring dermal wound healing after mesenchymal stem cell transplantation using nonlinear optical microscopy. Tissue Eng Part C Methods **16,** 1107, 2010.
89. Ntziachristos, V., Bremer, C., and Weissleder, R. Fluorescence imaging with near-infrared light: new technological advances that enable *in vivo* molecular imaging. Eur Radiol **13,** 195, 2003.
90. Kim, S.H., Lee, J.H., Hyun, H., Ashitate, Y., Park, G., Robichaud, K., Lunsford, E., Lee, S.J., Khang, G., and Choi, H.S. Near-infrared fluorescence imaging for noninvasive trafficking of scaffold degradation. Sci Rep **3,** 1198, 2013.
91. Cowles, E.A., Kovar, J.L., Curtis, E.T., Xu, H., and Othman, S.F. Near-infrared optical imaging for monitoring the regeneration of osteogenic tissue-engineered constructs. Biores Open Access **2,** 186, 2013.
92. Podoleanu, A.G. Optical coherence tomography. Br J Radiol **78,** 976, 2005.
93. Chen, C.-W., Betz, M.W., Fisher, J.P., Paek, A., and Chen, Y. Macroporous hydrogel scaffolds and their characterization by optical coherence tomography. Tissue Eng Part C Methods **17,** 101, 2010.
94. Okamura, T., Onuma, Y., García-García, H.M., Regar, E., Wykrzykowska, J.J., Koolen, J., Thuesen, L., Windecker, S., Whitbourn, R., and McClean, D.R. 3-Dimensional optical coherence tomography assessment of jailed side branches by bioresorbable vascular scaffoldsa proposal for classification. JACC Cardiovasc Interv **3,** 836, 2010.
95. Brugaletta, S., Radu, M.D., Garcia-Garcia, H.M., Heo, J.H., Farooq, V., Girasis, C., van Geuns, R.-J., Thuesen, L., McClean, D., and Chevalier, B. Circumferential evaluation of the neointima by optical coherence tomography after ABSORB bioresorbable vascular scaffold implantation: can the scaffold cap the plaque?. Atherosclerosis **221,** 106, 2012.
96. Gomez-Lara, J., Brugaletta, S., Diletti, R., Garg, S., Onuma, Y., Gogas, B.D., van Geuns, R.J., Dorange, C., Veldhof, S., and Rapoza, R. A comparative assessment by optical coherence tomography of the performance of the first and second generation of the everolimus-eluting bioresorbable vascular scaffolds. Eur Heart J **32,** 294, 2011.
97. Onuma, Y., Serruys, P.W., Perkins, L.E., Okamura, T., Gonzalo, N., García-García, H.M., Regar, E., Kamberi, M., Powers, J.C., and Rapoza, R. Intracoronary optical coherence tomography and histology at 1 month and 2, 3, and 4 years after implantation of everolimus-eluting bioresorbable vascular scaffolds in a porcine coronary artery modelclinical perspective an attempt to decipher the human optical coherence tomography images in the ABSORB trial. Circulation **122,** 2288, 2010.
98. Weissleder R., and Pittet, M.J. Imaging in the era of molecular oncology. Nature **452,** 580, 2008.
99. O'Neill, K., Lyons, S.K., Gallagher, W.M., Curran, K.M., and Byrne, A.T. Bioluminescent imaging: a critical tool in pre-clinical oncology research. J Pathol **220,** 317, 2010.
100. Vilalta, M., Jorgensen, C., Dégano, I.R., Chernajovsky, Y., Gould, D., Noël, D., Andrades, J.A., Becerra, J., Rubio, N., and Blanco, J. Dual luciferase labelling for non-invasive bioluminescence imaging of mesenchymal stromal cell chondrogenic differentiation in demineralized bone matrix scaffolds. Biomaterials **30,** 4986, 2009.
101. Geuze, R.E., Prins, H.-J., Öner, F.C., van der Helm, Y.J., Schuijff, L.S., Martens, A.C., Kruyt, M.C., Alblas, J., and Dhert, W.J. Luciferase labeling for multipotent stromal cell tracking in spinal fusion versus ectopic bone tissue engineering in mice and rats. Tissue Eng Part A **16,** 3343, 2010.
102. Liu, J., Barradas, A., Fernandes, H., Janssen, F., Papenburg, B., Stamatialis, D., Martens, A., van Blitterswijk, C., and de Boer, J. *In vitro* and *in vivo* bioluminescent imaging of hypoxia in tissue-engineered grafts. Tissue Eng Part C Methods **16,** 479, 2009.
103. Cresce, A.v.W., Dandu, R., Burger, A., Cappello, J., and Ghandehari, H. Characterization and real-time imaging of gene expression of adenovirus embedded silk-elastinlike protein polymer hydrogels. Mol Pharm **5,** 891, 2008.
104. Bagó, J.R., Aguilar, E., Alieva, M., Soler-Botija, C., Vila, O.F., Claros, S., Andrades, J.A., Becerra, J., Rubio, N., and Blanco, J. *In vivo* bioluminescence imaging of cell differentiation in biomaterials: a platform for scaffold development. Tissue Eng Part A **19,** 593, 2012.
105. Bai, X., Yan, Y., Coleman, M., Wu, G., Rabinovich, B., Seidensticker, M., and Alt, E. Tracking long-term survival of intramyocardially delivered human adipose tissue-derived stem cells using bioluminescence imaging. Mol Imaging Biol **13,** 633, 2011.

106. Emelianov, S.Y., Li, P.-C., and O'Donnell, M. Photoacoustics for molecular imaging and therapy. Phys Today **62,** 34, 2009.
107. Wang L.V., and Hu, S. Photoacoustic tomography: *in vivo* imaging from organelles to organs. Science **335,** 1458, 2012.
108. Cox, B., Laufer, J.G., Arridge, S.R., and Beard, P.C. Quantitative spectroscopic photoacoustic imaging: a review. J Biomed Opt **17,** 0612021, 2012.
109. Luke, G.P., Yeager, D., and Emelianov, S.Y. Biomedical applications of photoacoustic imaging with exogenous contrast agents. Ann Biomed Eng **40,** 422, 2012.
110. Nam, S.Y., Ricles, L.M., Suggs, L.J., and Emelianov, S.Y. Nonlinear photoacoustic signal increase from endocytosis of gold nanoparticles. Opt Lett **37,** 4708, 2012.
111. Cai, X., Paratala, B.S., Hu, S., Sitharaman, B., and Wang, L.V. Multiscale photoacoustic microscopy of single-walled carbon nanotube-incorporated tissue engineering scaffolds. Tissue Eng Part C Methods **18,** 310, 2011.
112. Zhang, Y., Cai, X., Choi, S.-W., Kim, C., Wang, L.V., and Xia, Y. Chronic label-free volumetric photoacoustic microscopy of melanoma cells in three-dimensional porous scaffolds. Biomaterials **31,** 8651, 2010.
113. Zhang, Y., Cai, X., Wang, Y., Zhang, C., Li, L., Choi, S.W., Wang, L.V., and Xia, Y. Noninvasive photoacoustic microscopy of living cells in two and three dimensions through enhancement by a metabolite dye. Angew Chem Int Ed Engl **123,** 7497, 2011.
114. Chung, E., Nam, S.Y., Ricles, L.M., Emelianov, S.Y., and Suggs, L.J. Evaluation of gold nanotracers to track adipose-derived stem cells in a PEGylated fibrin gel for dermal tissue engineering applications. Int J Nanomed **8,** 325, 2013.
115. Cai, X., Zhang, Y., Li, L., Choi, S.-W., MacEwan, M.R., Yao, J., Kim, C., Xia, Y., and Wang, L.V. Investigation of neovascularization in three-dimensional porous scaffolds *in vivo* by a combination of multiscale photoacoustic microscopy and optical coherence tomography. Tissue Eng Part C Methods **19,** 196, 2012.
116. Zhang, Y.S., Cai, X., Yao, J., Xing, W., Wang, L.V., and Xia, Y. Non-invasive and *in situ* characterization of the degradation of biomaterial scaffolds by volumetric photoacoustic microscopy. Angew Chem Int Ed Engl **53,** 184, 2014.
117. Talukdar, Y., Avti, P.K., Sun, J., and Sitharaman, B. Multimodal ultrasound-photoacoustic imaging of tissue engineering scaffolds and blood oxygen saturation in and around the scaffolds. Tissue Eng Part C Methods **20,** 440, 2014.
118. Nam, S.Y., Ricles, L.M., Suggs, L.J., and Emelianov, S.Y. *In vivo* ultrasound and photoacoustic monitoring of mesenchymal stem cells labeled with gold nanotracers. PLoS One **7,** e37267, 2012.
119. Ricles, L.M., Nam, S.Y., Sokolov, K., Emelianov, S.Y., and Suggs, L.J. Function of mesenchymal stem cells following loading of gold nanotracers. Int J Nanomed **6,** 407, 2011.
120. Kim, J., Piao, Y., and Hyeon, T. Multifunctional nanostructured materials for multimodal imaging, and simultaneous imaging and therapy. Chem Soc Rev **38,** 372, 2009.
121. Lee, D.-E., Koo, H., Sun, I.-C., Ryu, J.H., Kim, K., and Kwon, I.C. Multifunctional nanoparticles for multimodal imaging and theragnosis. Chem Soc Rev **41,** 2656, 2012.
122. Kempen, D.H.R., Yaszemski, M.J., Heijink, A., Hefferan, T.E., Creemers, L.B., Britson, J., Maran, A., Classic, K.L., Dhert, W.J.A., and Lu, L.C. Non-invasive monitoring of BMP-2 retention and bone formation in composites for bone tissue engineering using SPECT/CT and scintillation probes. J Control Release **134,** 169, 2009.
123. von Schulthess, G.K., Steinert, H.C., and Hany, T.F. Integrated PET/CT: current applications and future directions. Radiology **238,** 405, 2006.
124. Rodenberg, E., Azhdarinia, A., Lazard, Z.W., Hall, M., Kwon, S.K., Wilganowski, N., Salisbury, E.A., Merched-Sauvage, M., Olmsted-Davis, E.A., and Sevick-Muraca, E.M. Matrix metalloproteinase-9 is a diagnostic marker of heterotopic ossification in a murine model. Tissue Eng Part A **17,** 2487, 2011.
125. Gildehaus, F.J., Haasters, F., Drosse, I., Wagner, E., Zach, C., Mutschler, W., Cumming, P., Bartenstein, P., and Schieker, M. Impact of indium-111 oxine labelling on viability of human mesenchymal stem cells *in vitro*, and 3D cell-tracking using SPECT/CT *in vivo*. Mol Imaging Biol **13,** 1204, 2011.
126. Alric, C., Taleb, J., Duc, G.L., Mandon, C., Billotey, C., Meur-Herland, A.L., Brochard, T., Vocanson, F., Janier, M., and Perriat, P. Gadolinium chelate coated gold nanoparticles as contrast agents for both X-ray computed tomography and magnetic resonance imaging. J Am Chem Soc **130,** 5908, 2008.
127. Torres Martin de Rosales, R., Tavaré, R., Paul, R.L., Jauregui-Osoro, M., Protti, A., Glaria, A., Varma, G., Szanda, I., and Blower, P.J. Synthesis of 64CuII–bis (dithiocarbamatebisphosphonate) and its conjugation with superparamagnetic iron oxide nanoparticles: *in vivo* evaluation as dual-modality PET–MRI agent. Angew Chem Int Ed Engl **50,** 5509, 2011.
128. Jang, E.S., Lee, S.Y., Cha, E.-J., Sun, I.-C., Kwon, I.C., Kim, D., Kim, Y.I., Kim, K., and Ahn, C.-H. Fluorescent dye labeled iron oxide/silica core/shell nanoparticle as a multimodal imaging probe. Pharm Res 1, 2014.
129. Xu, H., Cheng, L., Wang, C., Ma, X., Li, Y., and Liu, Z. Polymer encapsulated upconversion nanoparticle/iron oxide nanocomposites for multimodal imaging and magnetic targeted drug delivery. Biomaterials **32,** 9364, 2011.
130. Cheng, L., Wang, C., Ma, X., Wang, Q., Cheng, Y., Wang, H., Li, Y., and Liu, Z. Multifunctional upconversion nanoparticles for dual-modal imaging-guided stem cell therapy under remote magnetic control. Adv Funct Mater **23,** 272, 2013.
131. Emelianov, S., Aglyamov, S., Karpiouk, A., Mallidi, S., Park, S., Sethuraman, S., Shah, J., Smalling, R., Rubin, J., and Scott, W. 1E-5 synergy and applications of combined ultrasound, elasticity, and photoacoustic imaging. Ultrasonics Symposium, 2006. IEEE, 2006, pp. 405.
132. Hannah, A., Luke, G., Wilson, K., Homan, K.A., and Emelianov, S. Indocyanine green-loaded photoacoustic nanodroplets–dual contrast nanoconstructs for enhanced photoacoustic and ultrasound imaging. ACS Nano **8,** 250, 2014.

Address correspondence to:
Stanislav Y. Emelianov, PhD
Department of Biomedical Engineering
The University of Texas at Austin
107 W. Dean Keeton St., C0800
Austin, TX 78712

E-mail: emelian@mail.utexas.edu

Received: March 31, 2014
Accepted: July 8, 2014
Online Publication Date: August 18, 2014